Novel $La_2O_2S:Eu^{3+}$ nanofibers fabricated from sulfurization of $La_2O_3:Eu^{3+}$ electrospun nanofibers

FEI BI[a], LIYAN WANG[a,*], JIAQI LI[b], GUANGQING GAI[a], XIANGTING DONG[b,*]

[a]*Laboratory of Building Energy-Saving Technology Engineering, College of Material Science and Engineering, Jilin Jianzhu University, Changchun 130118, China*

[b]*Key Laboratory of Applied Chemistry and Nanotechnology at Universities of Jilin Province, Changchun University of Science and Technology, Changchun 130022, China*

$La_2O_2S:Eu^{3+}$ nanofibers were successfully fabricated by electrospinning combined with a double-crucible sulfurization technique. X-ray powder diffraction (XRD) analysis indicated that $La_2O_2S:Eu^{3+}$ nanofibers were pure hexagonal phase with space group P-3m1. Scanning electron microscope (SEM) analysis and histograms revealed that the mean diameter of $La_2O_2S:Eu^{3+}$ nanofibers was 133.61±16.00 nm under the 95% confidence level. Photoluminescence (PL) analysis manifested that the $La_2O_2S:Eu^{3+}$ nanofibers emitted red emission at 624 nm attributed to $^5D_0 \rightarrow {}^7F_2$ energy levels transition of Eu^{3+} ions under the excitation of 264 nm ultraviolet light. It was found that the optimum molar ratio of Eu^{3+} ions was 5%. CIE analysis demonstrated that the emitting colors of $La_2O_2S:Eu^{3+}$ nanofibers were located in the yellow and red regions and color-tuned luminescence can be obtained by changing doping concentration of Eu^{3+} ions, which could be applied in the field of optical telecommunication and optoelectronic devices. The possible formation mechanism of $La_2O_2S:Eu^{3+}$ nanofibers were also proposed.

(Received July 11, 2019; accepted April 9, 2020)

Keywords: Lanthanum oxysulfide, Luminescence, Nanofibers, Electrospinning

1. Introduction

In recent years, electrospinning technology has been extensively explored as a simple and versatile method for forming inorganic superfine nanofibers using polymer/inorganic composite as the precursor [1-3]. The morphology of materials can be controlled by adjusting experimental conditions, such as the viscosity of spinning solution, relative air humidity, the structure of spinneret, spinning voltage, and the distance between the spinneret and the collector. Advantages of this novel process for fabricating 1D nanostructures include, but is not limited to, low cost, high efficiency and convenient assembly. It has been reported that the nanofibers was successfully synthesized *via* electrospinning [4-10].

Nanomaterials have been extensively studied because of their distinctive geometries, novel physical and chemical properties, and potential applications in nanoscale optical and electric devices [11-13]. Among these nanomaterials, nanofiber is a new kind of one-dimensional nanomaterials with special morphology. It has attracted increasing interest of scientists owing to its anisotropy, large length-to-diameter ratio, unique optical, electrical and magnetic performances [14-16]. Research on the fabrication and properties of nanofibers has become one of the popular subjects of study in the realm of nanomaterials.

The lanthanide (La-Lu) oxysulfides are known as wide-gap (4.6-4.8 eV) materials suitable for doping ions activation [17-19]. In addition, compared with the lanthanide oxides, oxysulfide is a more efficient phosphor with a broader excitation band. Therefore, the lanthanide oxysulfides become a very important host of inorganic materials which have high potential for applications in various fields, such as color television picture tubes, radiographic imaging, field emission displays, and long-lasting phosphorescence [20-22]. RE oxysulfides are more biocompatible than RE oxide, may be used as biological probe and label. Eu^{3+} is a hypersensitive activator to study local symmetry and local environmental. As an efficient red light phosphor, however, Eu^{3+}-doped La_2O_2S nanomaterials were given rather little attention. The reason might be that the La_2O_2S nanomaterials could not be prepared easily. Obtaining bulk $La_2O_2S:Eu^{3+}$ with good quality is not an easy task. Various routes have been explored to synthesize such useful materials. Conventionally, Ln_2O_2S (Ln=Y, La, Gd) were prepared by combustion reactions from mixed metal nitrate reactants and dithiooxamide $(CSNH_2)_2$ with ignition temperatures of 300-350 °C [23]. Pure-phase nanowires of Ln_2O_2S, $Ln_2O_2S_2$, and LnS_2 have been prepared through shape retention of the same starting $Ln(OH)_3$ (Ln=La or Nd) nanowires *via* a boron-sulfur method at 400-500 °C for 10 min or 24 h [24]. In addition, the Eu-doped La_2O_2S

phosphor materials were prepared by annealing the mixture of rare-earth oxides, sulfur and Na_2CO_3 at 1000 °C [25].

In this study, pure hexagonal phase $La_2O_2S:Eu^{3+}$ nanofibers were prepared through calcining the electrospun PVP/[$La(NO_3)_3$+$Eu(NO_3)_3$] composite nanofibers, and then $La_2O_2S:x\%Eu^{3+}$[x stands for molar ratio of Eu^{3+} to (La^{3+}+Eu^{3+}), x=1, 3, 5 and 7] nanofibers were fabricated by sulfurization of $La_2O_3:x\%Eu^{3+}$ nanofibers *via* a double-crucible method we newly proposed for the first time. The samples were systematically characterized using modern measurements techniques. A possible formation mechanism of $La_2O_2S:Eu^{3+}$ nanofibers was also presented and some meaningful results were obtained.

2. Experimental sections

2.1. Chemicals

Polyvinyl pyrrolidone (PVP) (Mw=1 300 000, AR) was bought from Tiantai Chemical Co. Ltd. Yttrium oxide (La_2O_3, 99.99%) and europium oxide (Eu_2O_3, 99.99%) were purchased from Kemiou Chemical Co.,Ltd. N, N-dimethylformamide (DMF, AR) and Sulfur powder (S, AR) were purchased from Sinopharm Chemical Reagent Co. Ltd. Nitric acid (HNO_3, AR) was bought from Beijing Chemical Works. All chemicals were directly used as received without further purification.

2.2. Preparation of PVP/[$La(NO_3)_3$+$Eu(NO_3)_3$] composite nanofibers *via* electrospinning

In the typical procedure of preparing representative $La_2O_3:5\%Eu^{3+}$ nanobelts, 1.712 g of La_2O_3 and 0.097 g of Eu_2O_3 were dissolved in dilute HNO_3 (1:1, volume ratio) at elevated temperature, then rare earth nitrates were obtained by heating. 14.6 g of DMF, and 3.0 g of PVP were added into the above solution under stirring for 10 h to form homogeneous transparent precursor solution. In the precursor solution, the mass ratios of rare earth nitrates, DMF and PVP were equal to 12:73:15. Subsequently, the precursor solution was electrospun at room temperature under a positive high voltage of 18 kV, the distance between the capillary tip and the collector (Aluminium foil) was fixed to 18 cm, and relative humidity was 50%-60%. PVP/[$La(NO_3)_3$+$Eu(NO_3)_3$] composite nanofibers were obtained on the collector. Other series of $La_2O_3:x\%Eu^{3+}$ (x=1, 3 and 7) nanofibers were prepared by the similar procedure except for different doping molar concentration of Eu^{3+}.

2.3. Fabrication of $La_2O_3:Eu^{3+}$ nanofibers

The above PVP/[$La(NO_3)_3$+$Eu(NO_3)_3$] composite nanofibers were calcined at 700 ºC for 8 h with a heating rate of 1 ºC/min. Then the calcination temperature was decreased to 200 ºC at a rate of 1 ºC/min. Finally, samples were naturally cooled down to room temperature and $La_2O_3:Eu^{3+}$ nanofibers were obtained.

2.4. Synthesis of $La_2O_2S:Eu^{3+}$ nanofibers

$La_2O_3:Eu^{3+}$ hollow nanofibers were loaded into a small crucible. A few carbon rods were put into a big crucible, and then the small crucible was placed into the big crucible. Next, some sulphur powders were loaded into the space between the two crucibles, and then the big crucible was covered with its lid. We call this process a double-crucible method. Finally the crucibles were annealed at 800 ºC for 4 h under argon atmosphere, and then the temperature was decreased to 200 ºC at a rate of 1 ºC/min followed by natural cooling down to ambient temperature. Thus, $La_2O_2S:Eu^{3+}$ nanofibers were obtained.

2.5. Characterization methods

The X-ray diffraction (XRD) measurement was performed using a Rigaku D/max-RA XRD diffractometer with Cu Kα line of 0.15418 nm. The field emission scanning electron microscope (FESEM, XL-30, FEI Company) was used to characterize the morphologies and sizes of the products. The distribution histograms of diameters were drawn by Image-Pro Plus 6.0 and Origin 8.5 softwares. The excitation and emission spectra of samples were recorded with a HITACHI F-7000 fluorescence spectrophotometer using a Xe lamp as the excitation source. All the experiments were performed at room temperature.

3. Results and discussion

3.1. Characterizations of structure and morphology

Fig. 1 reveals the XRD patterns of $La_2O_2S:Eu^{3+}$ nanofibers. The XRD analysis result of $La_2O_2S:Eu^{3+}$ nanofibers demonstrates that the characteristic diffraction peaks of the samples can be easily indexed to those of the pure hexagonal phase with primitive structure of La_2O_2S (PDF#71-2098), and the space group is P-3m1. In addition, with the increase of the concentration of Eu^{3+}, no obvious shifting of peaks can be detected, indicating that La^{3+} may be substituted by Eu^{3+} successfully to form the luminescence center because of the similar radius between La^{3+} and Eu^{3+}. No peaks of any other phases or impurities are also detected, indicating that crystalline $La_2O_2S:Eu^{3+}$ were acquired *via* sulfurization of crystalline $La_2O_3:Eu^{3+}$.

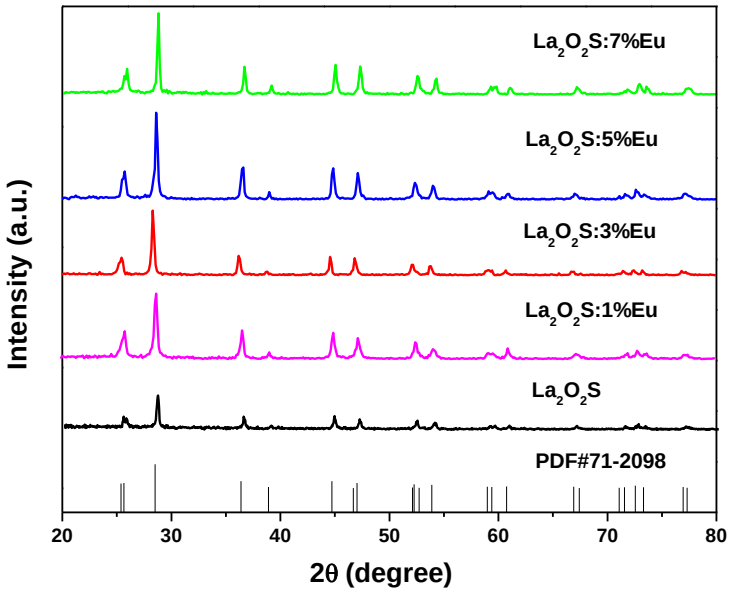

Fig. 1. XRD patterns of $La_2O_2S:x\%Eu^{3+}$ (x=0, 1, 3, 5 and 7) nanofibers (color online)

Fig. 2 shows the representative SEM images of the PVP/[$La(NO_3)_3$+$Eu(NO_3)_3$] composite nanofibers, $La_2O_3:Eu^{3+}$ nanofibers and $La_2O_2S:Eu^{3+}$ nanofibers. From the SEM image of Fig. 2a, it can be noticed that the PVP/[$La(NO_3)_3$+$Eu(NO_3)_3$] composite nanofibers have smooth surface and uniform diameter with good dispersivity. Fig. 2b indicates the SEM image of as-prepared $La_2O_3:Eu^{3+}$ nanofibers. It can be clearly seen that the morphology of nanofibers have relatively smooth surface by calcination of the respective electrospun PVP/[$La(NO_3)_3$+$Eu(NO_3)_3$] composite nanofibers. After annealing and sulfurization at 800 °C, as-formed $La_2O_2S:Eu^{3+}$ nanofibers have coarse surface, as revealed in Fig. 2c. From Fig. 2c, one can see that the sample exhibits fibrous structure. It reveals that $La_2O_2S:Eu^{3+}$ nanofibers retain their 1D morphology. From above analyses, we can safely conclude that the sulfurization technique we proposed here can retain the morphology of the precursor nanofibers.

Under the 95 % confidence level, the diameters of PVP/[$La(NO_3)_3$+$Eu(NO_3)_3$] composite nanofibers, $La_2O_3:Eu^{3+}$ nanofibers and $La_2O_2S:Eu^{3+}$ nanofibers analyzed by Shapiro-Wilk method are normal distribution. Distribution histograms of diameters of the samples are indicated in Fig. 3. As seen from Fig. 3, the diameters of PVP/[$La(NO_3)_3$+$Eu(NO_3)_3$] composite nanofibers, $La_2O_3:Eu^{3+}$ nanofibers and $La_2O_2S:Eu^{3+}$ nanofibers are 394.86±53.11 nm, 172.75±21.44 nm and 133.61±16.00 nm, respectively.

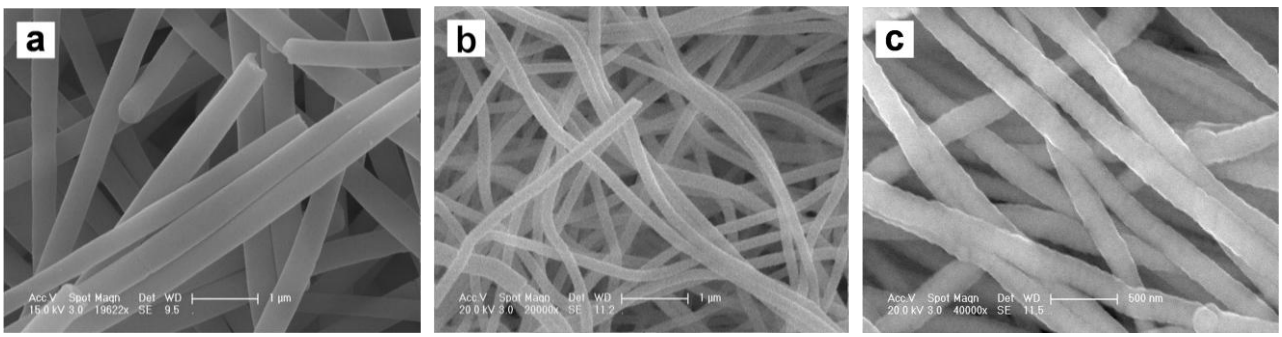

Fig. 2. SEM images of PVP/[$La(NO_3)_3$+$Eu(NO_3)_3$] composite nanofibers (a), $La_2O_3:Eu^{3+}$ nanofibers (b) and $La_2O_2S:Eu^{3+}$ nanofibers (c)

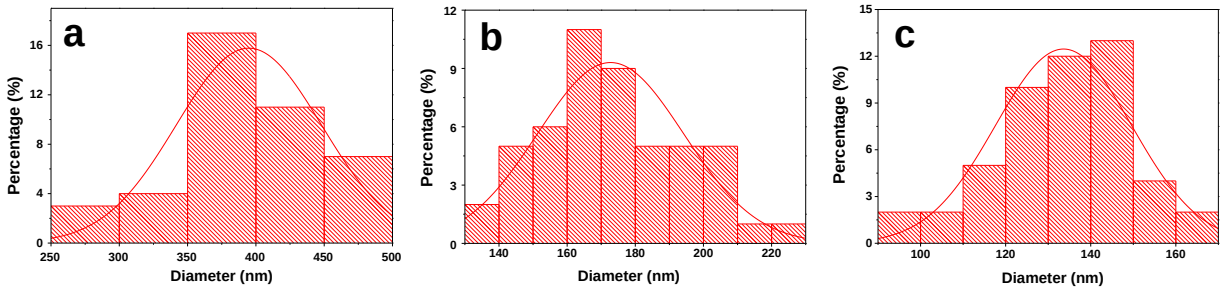

Fig. 3. Distribution histograms of diameters of PVP/[$La(NO_3)_3$+$Eu(NO_3)_3$] composite nanofibers (a), La_2O_3:Eu^{3+} nanofibers (b) and La_2O_2S:Eu^{3+} nanofibers (c)

3.2. Photoluminescence properties

Fig. 4 shows the excitation (monitored by 624 nm) and emission (excited by 264 nm) spectra of La_2O_2S:x%Eu^{3+} (x=1, 3, 5 and 7) nanofibers. The excitation spectra (Fig. 4a) exhibits one strong broadband in the range from 200 to 300 nm with a maximum at 264 nm, which is associated to the CT absorption of the 2p orbital of O^{2-} ions to the 4f orbital of Eu^{3+}. And small peak around 324 nm in Fig. 4a is attributed to the CT transition from 2p orbital of S^{2-} ions to the 4f orbital of Eu^{3+} ions [21]. The emission spectra of La_2O_2S:x%Eu^{3+} (x=1, 3, 5 and 7) nanofibers is shown in the Fig. 4b. It is found from Fig. 4b that the emission peaks consist of several peaks at 537 nm ($^5D_1\rightarrow{}^7F_1$), 555 nm ($^5D_1\rightarrow{}^7F_2$), 587 nm ($^5D_0\rightarrow{}^7F_0$), 594 nm ($^5D_0\rightarrow{}^7F_1$), 616 nm ($^5D_0\rightarrow{}^7F_2$) and 624 nm ($^5D_0\rightarrow{}^7F_2$) which originate from the energy levels transitions of Eu^{3+} ions, respectively. Among these emission peaks, the red emission at 624 nm attributed to $^5D_0\rightarrow{}^7F_2$ energy levels transition of Eu^{3+} ions is the strongest one.

Fig. 4 demonstrates the PL spectra of La_2O_2S:Eu^{3+} nanofibers with different doping concentrations of Eu^{3+} ions. It is found that the spectral shape and locations of excitation and emission peaks do not vary with the doping concentrations of Eu^{3+} ions for La_2O_2S:Eu^{3+} nanofibers, but the intensity of excitation and emission peaks for La_2O_2S:Eu^{3+} nanofibers strongly depend on the doping concentration of Eu^{3+} ions, and the strongest excitation and emission spectra can be obtained when the doping molar concentration of Eu^{3+} is 5%. Obviously, the luminescence intensity of La_2O_2S:Eu^{3+} nanofibers increases with the increase of the concentration of Eu^{3+} from the beginning, reaches a maximum value with the Eu^{3+} concentration of 5%, and then decreases with further increase in Eu^{3+} concentration.

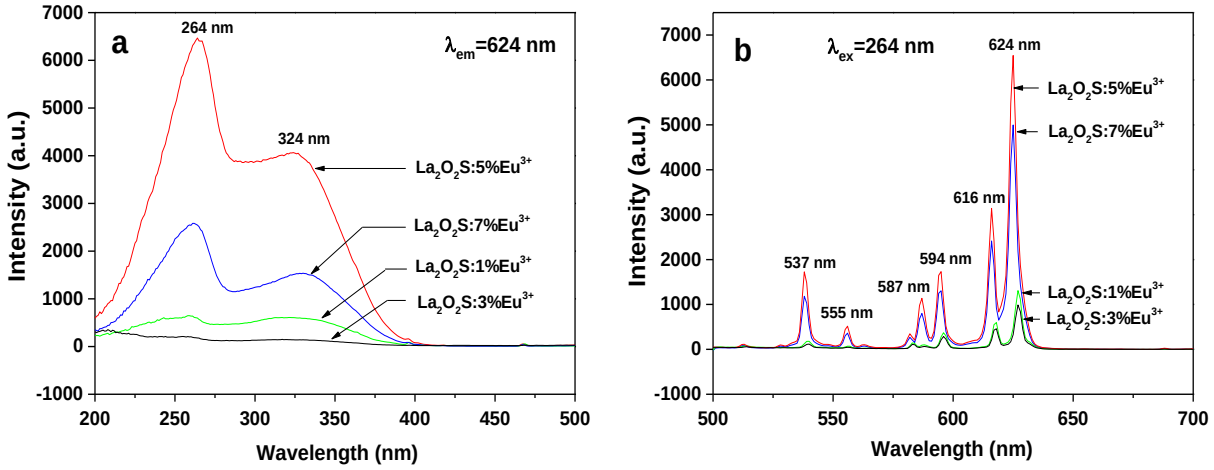

Fig. 4. Excitation (a) and emission (b) spectra of the La_2O_2S:x%Eu^{3+} (x=1, 3, 5 and 7) nanofibers (color online)

PL decay curves of La_2O_2S:x%Eu^{3+} (x=1, 3, 5 and 7) nanofibers with different concentrations of Eu^{3+} shown in Fig. 5, are used to calculate the lifetime and to investigate the luminescence dynamics of these samples. The samples are excited by 264 nm and monitored at 624 nm. It can be seen that all the curves can be well-fitted into a single-exponential function as $I_t=I_0exp(-t/\tau)$, where I_t is the intensity at time τ, I_0 is the intensity at t=0, and τ is the decay lifetime. With the help of the software Origin 8.5, the values of τ can be obtained. The average lifetime of La_2O_2S:x%Eu^{3+} (x=1, 3, 5 and 7) nanofibers are 0.84 ms, 0.87 ms, 1.02 ms and 0.89 ms, respectively.

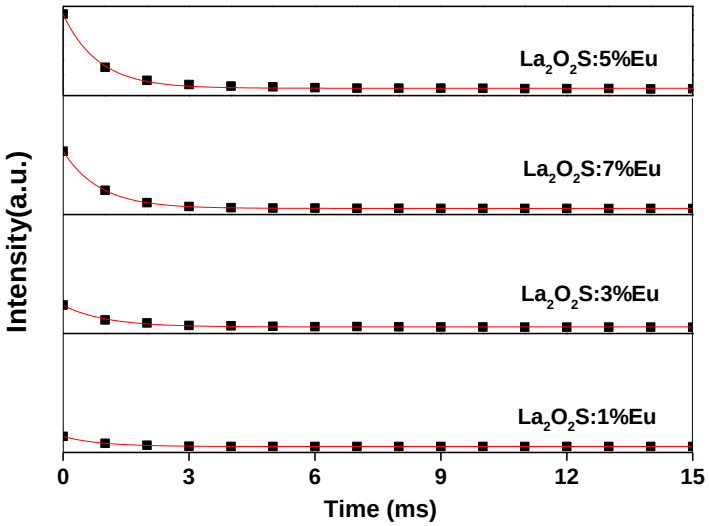

Fig. 5. Luminescence decay curves of $La_2O_2S:x\%Eu^{3+}$ (x=1, 3, 5 and 7) nanofibers

3.3. CIE analysis

Generally, color is represented by the Commission Internationale de L'Eclairage (CIE) chromaticity coordinates and color ratios. The chromaticity coordinates and color ratios have been calculated from the emission spectra by the method described in previous report [1, 2]. For the $La_2O_2S:x\%Eu^{3+}$ (x=1, 3, 5 and 7) nanofibers, the chromaticity coordinates (X, Y) are determined to be (0.5584, 0.4271), (0.5600, 0.269), (0.5896, 0.4058) and (0.5939, 0.4016), respectively. Remarkably, the emission colors of $La_2O_2S:x\%Eu^{3+}$ (x=1, 3, 5 and 7) nanofibers shift from yellow to red along with the variation of concentrations of Eu^{3+}, as shown in Fig. 6. These results indicate that the color emissions can be tuned by changing the concentration of doping activator ions. These as-obtained nanostructures could show merits of red emissions, which is considered to be a promising candidate for application in LEDs.

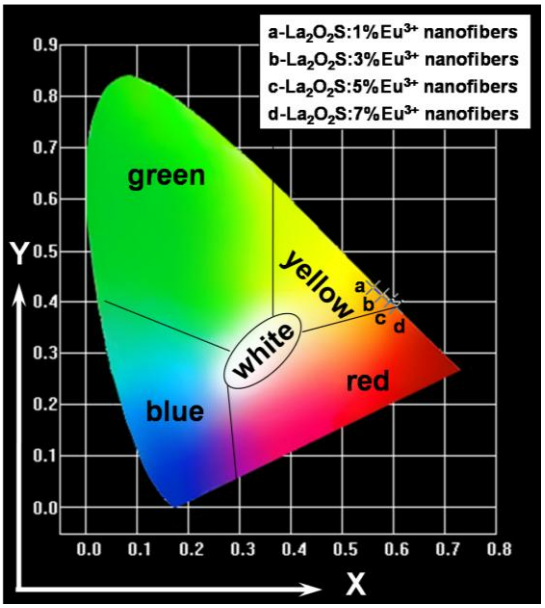

Fig. 6. CIE chromaticity coordinates diagram of $La_2O_2S:x\%Eu^{3+}$ (x=1, 3, 5 and 7) nanofibers (color online)

3.4. Formation mechanism for $La_2O_2S:Eu^{3+}$ nanofibers

The formation mechanism for $La_2O_2S:Eu^{3+}$ nanofibers is proposed on the basis of the above experiment results, as shown in Fig. 7. PVP, $La(NO_3)_3$ and $Eu(NO_3)_3$ were mixed with DMF to form precursor solution with certain viscosity. Then, PVP/[$La(NO_3)_3$+$Eu(NO_3)_3$] composite nanofibers were obtained *via* electrospinning. The viscosity of the spinning solution for fabricating nanofibers was lower, and the applied voltage was higher, the spinning velocity was faster. The charge repulsion force acted on the radial direction of the jets had time to stretch the jets into fiber shape, resulted in the formation of composite nanofibers. The morphologies of the composite nanostructures were basically retained after performing the following calcination process. Some solvent was volatilized in the electrospinning process. During calcination process, PVP chain was broken and volatilize. The La^{3+}, Eu^{3+} and NO_3^- ions moved to the surface of the composite fibers with evaporation of solvent DMF. With the increase in calcination temperature, nitrates were decomposed and oxidized to NO_2, La^{3+} and Eu^{3+} were oxidized to form $La_2O_3:Eu^{3+}$ crystallites, many crystallites were combined into nanoparticles, then some nanoparticles were mutually connected to generate $La_2O_3:Eu^{3+}$ nanofibers. PVP acted as template during the formation of $La_2O_3:Eu^{3+}$ nanofibers. It was found from experiments that the average molecular weight of PVP and content of PVP in the precursor solution played important roles in the formation of $La_2O_3:Eu^{3+}$ nanofibers [6]. Next, $La_2O_3:Eu^{3+}$ nanofibers were sulfurized using sulfur powders as sulfurizing agent. During the process, sulfur powders and $La_2O_3:Eu^{3+}$ nanofibers were separated by the small crucible, which prevented $La_2O_3:Eu^{3+}$ nanofibers from morphology damage. If $La_2O_3:Eu^{3+}$ nanofibers were directly mixed with sulfur powders, melted sulfur will cut the $La_2O_3:Eu^{3+}$ nanofibers into pieces, as a result, the morphology of $La_2O_3:Eu^{3+}$ nanofibers cannot be retained [15]. Carbon rods played an important role in the reduction *via* combination with O_2 to produce CO, which react with oxygen species of $La_2O_3:Eu^{3+}$ to give CO_2 in the heating process. The double-crucible method we proposed here is actually a solid-gas reaction, which has been proved to be an important method, not only can retain the morphology of $La_2O_3:Eu^{3+}$ nanofibers, but also can fabricate $La_2O_2S:Eu^{3+}$ nanofibers with pure phase at relatively low temperature. Reaction schemes for formation of $La_2O_2S:Eu^{3+}$ nanofibers proceed as follows:

$$PVP/[La(NO_3)_3+Eu(NO_3)_3]+O_2 \xrightarrow{700\ ^\circ C} CO_2+H_2O+NO_2+La_2O_3:Eu^{3+} \quad (1)$$

$$C+O_2 \longrightarrow CO \quad (2)$$

$$La_2O_3:Eu^{3+}+S+CO \xrightarrow{800\ ^\circ C} La_2O_2S:Eu^{3+}+CO_2 \quad (3)$$

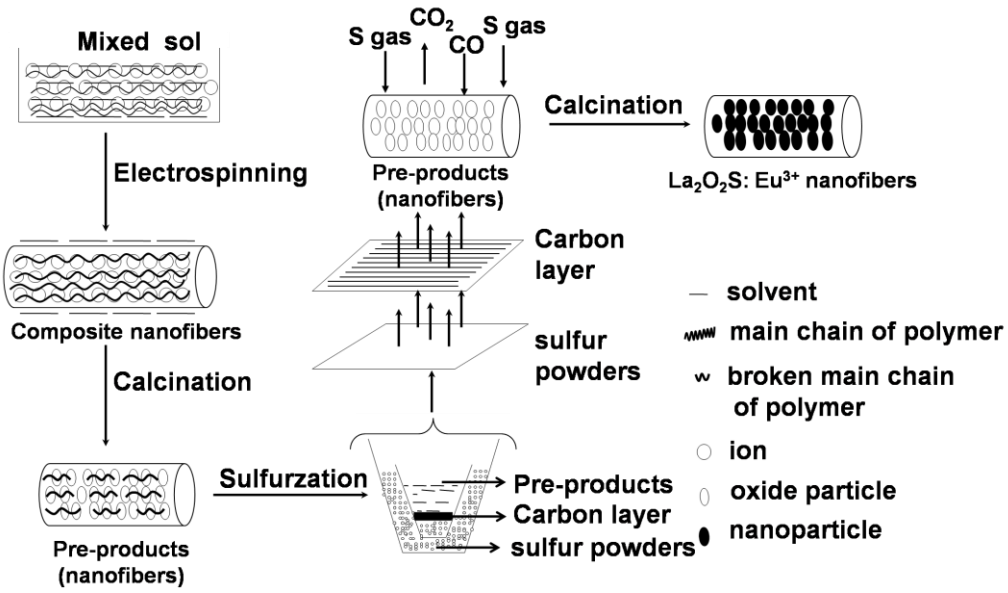

Fig. 7. Formation mechanism of $La_2O_2S:Eu^{3+}$ nanofibers

4. Conclusions

Pure hexagonal phase $La_2O_2S:Eu^{3+}$ nanofibers were successfully fabricated by sulfurization of the $La_2O_3:Eu^{3+}$ nanofibers. The morphology of $La_2O_2S:Eu^{3+}$ nanofibers can be inherited from $La_2O_3:Eu^{3+}$ nanofibers under the sulfurization circumstance *via* a double-crucible method we newly proposed. The surface of $La_2O_2S:Eu^{3+}$ nanofibers was coarse and the mean diameter of $La_2O_2S:Eu^{3+}$ nanofibers is 133.61±16.00 nm. Emission spectra analysis manifested that $La_2O_2S:Eu^{3+}$ nanofibers emitted red emission at 624 nm attributed to $^5D_0 \rightarrow {}^7F_2$ energy levels transition of Eu^{3+} ions. The double-crucible method we proposed here is of great importance. This technique can be employed to fabrication of other pure-phase rare earth oxysulfide nanomaterials with various morphologies.

Acknowledgements

This work was financially supported by the National Natural Science Foundation of China (NSFC 50972020, 51072026), Ph.D. Programs Foundation of the Ministry of Education of China (20102216110002, 20112216120003), the Science and Technology Development Planning Project of Jilin Province (Grant Nos. 20070402, 20060504), Key Research Project of Science and Technology of Ministry of Education of China (Grant No. 207026), the Science and Technology Research Project of the Education Department of Jilin Province during the thirteenth five-year plan period (Grant No. JJKH20180580KJ, JJKH20180582KJ) and the Scientific Development Program of Jilin Province (Grant No. 20170520152JH).

References

[1] F. Bi, X. T. Dong, J. X. Wang, G. X. Liu, J. Mater. Sci.: Mater. in Electron. **25**(10), 4259 (2014).
[2] W. W. Ma, X. T. Dong, J. X. Wang, W. S. Yu, G. X. Liu, J. Mater. Sci. **48**, 2557 (2013).
[3] M. Q. Chi, S. H. Chen, M. X. Zhong, C. Wang, X. F. Lu, Chem. Commun. **54**, 5827 (2018).
[4] Y. T. Geng, P. Zhang, Q. T. Wang, Y. X. Liu, K. Pan, J. Mater. Chem. B **5**, 5390 (2017).
[5] C. Luo, X. X. Wang, J. Q. Wang, K. Pan, Compos. Sci. Technol. **133**, 97 (2016).
[6] Q. L. Kong, J. X. Wang, X. T. Dong, W. S. Yu, G. X. Liu, J. Mater. Sci.: Mater. in Electron. **24**, 4745 (2013).
[7] Q. L. Ma, J. X. Wang, X. T. Dong, W. S. Yu, G. X. Liu, Adv. Funct. Mater. **25** (16), 2436 (2015).
[8] N. Lv, Z. Q. Wang, W. Z. Bi, G. M. Li, J. L. Zhang, J. Z. Ni, J. Mater. Chem. B **4**, 4402 (2016).
[9] Z. Y. Hou, G. G. Li, H. Z. Lian, J. Lin, J. Mater. Chem. **22** (12), 5254 (2012).
[10] Z. Y. Hou, P. P. Yang, C. X. Li, L. L. Wang, Chem. Mater. **20**(21), 6686 (2008).
[11] M. Gao, X. F. Lu, M. Q. Chi, S. H. Chen, C. Wang, Inorg. Chem. Front. **4**, 1862 (2017).
[12] J. Tian, Q. L. Ma, W. S. Yu, X. T. Dong, Y. Yang, B. Zhao, J. X. Wang, G. X. Liu, New J. Chem. **41**, 13983 (2017).
[13] N. Lv, J. L. Zhang, G. M. Li, X. Wang, J. Z. Ni, J. Phys. Chem. C **121**(21), 11926 (2017).
[14] X. F. Lu, C. Wang, Y. Wei, Small **5**, 2349 (2009).
[15] J. Zhao, Y. Yang, X. T. Dong, Q. L. Ma, W. S. Yu, J. X. Wang, G. X. Liu, RSC Advances **6**(69), 64741 (2016).
[16] S. Xu, X. L. Wang, X. T. Dong, W. S. Yu, J. X. Wang, G. X. Liu, RSC Advances **6**(49), 43322 (2016).
[17] L. Y. Yang, J. X. Wang, X. T. Dong, G. X. Liu, W. S. Yu, J. Mater. Sci. **48**, 644 (2013).
[18] G. D. Liu, Q. H. Zhang, H. Z. Wang, Y. G. Li, Mater. Sci. Eng. B **177**, 316 (2012).
[19] N. T. Lau, M. Fang, C. K. Chan, Appl. Catal. B: Environ. **79**, 110 (2018).
[20] M. Pokhrel, A. K. Gangadharan, D. K. Sardar, Mater. Lett. **99**, 86 (2013).
[21] S. V. Yap, R. M. Ranson, W. M. Cranton, D. C. Koutsogeorgis, G. B. Hix, J. Lumin. **129**, 416 (2009).
[22] Y. M. Yang, C. Mi, F. Yu, X. Y. Su, C. F. Guo, G. Li, J. Zhang, L. L. Liu, Y. Z. Liu, X. D. Li, Ceram. Int. **40**, 9875 (2014).
[22] J. Bang, M. Abboudi, B. Abrams, P. H. Holloway, J. Lumin. **106**, 177 (2004).
[23] Y. Z. Huang, L. Chen, L. M. Wu, Cryst. Growth Des. **8**(2), 739 (2008).
[24] J. J. Oh, B. K. Jin, W. J. Chung, D. W. Shin, Y. G. Choi, Curr. Appl. Phys. **11**, S15 (2011).

*Corresponding author: wlynzy@163.com;
dongxiangting888@163.com